Dental Materials Journal 2008; 27(3): 408–414

Original Paper

Mechanical Properties of Dental Zirconia Ceramics Changed with Sandblasting and Heat Treatment

Hideo SATO[1], Kiyotaka YAMADA[2], Giuseppe PEZZOTTI[2], Masahiro NAWA[3] and Seiji BAN[1]

[1]*Department of Biomaterials Science, Graduate School of Medical and Dental Sciences, Kagoshima University, 8-35-1 Sakuragaoka, Kagoshima 890-8544, Japan*

[2]*Ceramic Physics Laboratory and Research Institute for Nanoscience, Kyoto Institute of Technology, Sakyo-ku, Matsugasaki, Kyoto 606-8585, Japan*

[3]*Central Research Laboratory, Matsushita Electric Works, Ltd., 1048, Kadoma, Osaka 571-8686, Japan*

Corresponding author, Seiji BAN; E-mail: sban@denta.hal.kagoshima-u.ac.jp

Two types of tetragonal zirconia polycrystals (TZP), a ceria-stabilized TZP/Al_2O_3 nanocomposite (CZA) and a conventional yttria-stabilized TZP (Y-TZP), were sandblasted with 70-μm alumina and 125-μm SiC powders, then partially annealed at 500–1200℃ for five minutes. Monoclinic ZrO_2 content was determined by X-ray diffractometry and Raman spectroscopy. Biaxial flexure test was conducted on the specimens before and after the treatments. Monoclinic ZrO_2 content and biaxial flexure strength increased after sandblasting, but decreased after heat treatment. However, in both cases, the strength of CZA was higher than that of Y-TZP. Raman spectroscopy showed that a compressive stress field was introduced on the sample surface after sandblasting. It was concluded that sandblasting induced tetragonal-to-monoclinic phase transformation and that the volume expansion associated with such a phase transformation gave rise to an increase in compressive stress on the surface of CZA. With the occurrence of such a strengthening mechanism in the microstructure, it was concluded that CZA was more susceptible to stress-induced transformation than Y-TZP.

Key words: Zirconia, Sandblasting, Heat treatment

Received Nov 2, 2007: Accepted Nov 30, 2007

INTRODUCTION

The demand for metal-free restorations in dental practice has increased unabatedly because of two factors: strong esthetic demand and concern about metallic hypersensitivity[1]. To these delicate medical issues and challenges, zirconia is indicated as an optimal soltuion[2,3]. Tetragonal zirconia polycrystals (TZP), especially 3 mol% Y_2O_3-stabilized zirconia (3Y-TZP), has been used as a conventional material for medical and dental restorations. On the other hand, some researchers recently reported that a Ce-TZP/Al_2O_3 nanocomposite (CZA) not only exhibited higher strength, but might also have higher fracture toughness when compared with conventional Y-TZP[4,5].

By virtue of the abovementioned beneficial properties, zirconia-based materials are employed as core materials for crowns and bridges in restorative dentistry. On zirconia-based frameworks for crown and bridge restorations, fabrication using the CAD/CAM system is a standard routine[6,7].

After fabrication using CAD/CAM system and before veneering, one or more surface treatments are typically performed. In particular, sandblasting is an important treatment method to get a strong adhesion to veneering porcelain. However, mechanical stress is known to induce phase transformation from tetragonal to monoclinic ZrO_2, subsequently resulting in compressive stress[8-16]. Therefore, heat treatment is recommended after sandblasting in dental practice[17]. The aim of this study, therefore, was to examine the effects of sandblasting and heat treatment on dental zirconia ceramics.

MATERIALS AND METHODS

Disk specimen preparation

As listed in Table 1, two types of TZP ceramics were used in this study. CZA powder was processed by cold isostatic pressing method into a cylindrical rod, 19.5 mm in diameter and 100 mm in length. After peeling of the rod surface and firing at 1450℃ for two hours, disk-shaped specimens of two sizes, 14 mm in diameter/2 mm in thickness and 15 mm in diameter/0.5 mm in thickness, were prepared by cutting and grinding with a 400-grit diamond wheel.

Conventional Y-TZP was used for comparison in this study. Its powder was pressed using the same method. After firing at 1350℃ for six hours, disk-shaped specimens of two sizes were prepared in the same manner as CZA.

Sandblasting and heat treatment

All disk specimens (ϕ 14 mm /t 2 mm) were ground with diamond papers (#220, #400, #600, and #1000), and subsequently heated at 1200℃

Table 1 Materials used in this study

Code	Product Name (Manufacturer)	Composition	Final Sintering
CZA	NANOZR (Matsushita Electric Works)	10 mol% CeO_2-ZrO_2 30 vol.% Al_2O_3	1450℃, 2 hr
Y-TZP	TZ-3YB-E (Tosoh)	3 mol% Y_2O_3-ZrO_2	1350℃, 6 hr

for 10 minutes (Cerafusion VPF, Jelenko, MA, USA) to form homogeneous tetragonal ZrO_2. Disks were sandblasted by 70-μm alumina and 125-μm SiC powders for 10 and 90 seconds at 0.4 MPa air pressure at a direction perpendicular to the surface and at a distance 10 mm away (Hi-Blaster-II, Shofu, Kyoto, Japan). Part of the sandblasted specimens were heated at 500−1200℃ for five minutes.

Microscopic observation

Microscopic observation was conducted on both types of zirconia using a scanning electron microscope (SEM; JSM-5510LV, JEOL, Tokyo, Japan). It was operated at an accelerating voltage of 20 kV to investigate the surface geometry. To characterize the microstructure, the surfaces of CZA and Y-TZP before surface treatments were thermally etched at 1300℃ and 1200℃ respectively for one hour. To observe the effects of surface treatments on CZA and Y-TZP surfaces, grinding and sandblasting were performed.

Surface roughness measurement

Surface roughness of the specimens was analyzed using a surface roughness tester (Surfcom 130A, Accretech, Tokyo, Japan). Six measurements were performed for each specimen according to ISO 4287:1997. The arithmetical mean deviation of the assessed profile (Ra) and the maximum height of profile (Rz) were measured under these conditions: cut-off value of 0.8 mm, measurement length of 5.0 mm, and measurement speed of 0.6 mm/s. Filtering of the measured data was conducted using a Gaussian filter.

X-ray diffraction and Raman spectroscopy analyses

The amount of transformation which was induced by sandblasting and heat treatment was determined by measuring the peak intensity ratio in the X-ray diffraction (XRD) pattern of disk-shaped specimens (ϕ 14 mm /t 2 mm) of both zirconia types (n=3 per group). XRD data were collected with a $\theta/2\theta$ diffractometer (RINT-2500, Rigaku, Tokyo, Japan) using Cu-K_α = 1.54Å radiation at 40 kV and 120 mA. Diffractograms were obtained from 20° to 40° at a scan speed of 1°/min. Monoclinic peak intensity ratio, X_m, was calculated using the Garvie and Nicholson method[18] as follows:

$$X_m = \frac{I_m(\bar{1}11) + I_m(111)}{I_m(\bar{1}11) + I_m(111) + I_t(101)} \quad (1)$$

where I_t and I_m represent the integrated intensity (area under the peaks) of the tetragonal (101) and monoclinic (111) and (-111) peaks around 30°, 31°, and 28° respectively. Monoclinic volume content, V_m, was calculated using the method of Toraya *et al.*[19]:

$$V_m = \frac{1.311X_m}{1 + 0.311X_m} \quad (2)$$

Raman spectra were collected with a triple monochromator spectrometer (T-64000, ISA Jovin-Ivon/Horiba Group, Tokyo, Japan) equipped with a charge-coupled device detector (high-resolution CCD camera). In residual stress fields, the required laser power on the material surface was typically about 200 mW at the laser head. A suitable excitation frequency was a monochromatic blue line emitted by an Ar-ion laser at a wavelength of 488 nm. Spectral integration time was eight seconds, with the recorded spectra averaged over three successive measurements. Laser spot of 1 μm in diameter was always focused on the specimen surface. Raman peak positions were obtained by fitting the CCD raw data to mixed Gaussian/Lorentzian curves with a commercially available software.

CZA disk was placed on a mapping device (lateral resolution of 0.1 μm), which was connected to a personal computer to drive highly precise displacements (along both x and y axes) on the specimen surface with a confocal configuration. The monoclinic content of CZA phase, V_m, contained in a partly transformed zone, could be quantitatively evaluated from the relative intensities of selected non-overlapping Raman bands, which belonged to the tetragonal phase at 150 cm^{-1} and to the monoclinic phase at 180 cm^{-1} and 190 cm^{-1}. Monoclinic volume content, V_m, was then calculated using a method of Katagiri *et al.*[20]:

$$V_m = \frac{0.5\,(I_m^{180} + I_m^{190})}{2.2 I_t^{150} + 0.5\,(I_m^{180} + I_m^{190})} \quad (3)$$

where I_t and I_m represent the intensities of bands identified by their apexes. In addition, it is well known that Raman peak positions shift linearly with increasing stress. In view of this, the equilibrium stress σ_{eq} of CZA was calculated as follows:

$$\sigma_{eq} = V_A \cdot \sigma_A + V_Z \cdot (V_m \cdot \sigma_m + V_t \cdot \sigma_t) \quad (4)$$

where σ_A, σ_z, σ_m, and σ_t are the magnitudes of residual stresses within alumina, zirconia, monoclinic zirconia and tetragonal zirconia phases, respectively. V_A, V_z, V_m, and V_t are the local volume contents of individual phases with alumina, zirconia, monoclinic zirconia and tetragonal zirconia phases, respectively. These detections were performed on the outermost surface and to a depth of 50 μm along the z-axis[21]. More details on the experimental setup, calibration procedures, and stress calculations with Raman spectroscopy were as per described previosly[22,23].

Biaxial flexure test

Six specimens (ϕ 15mm /t 0.5 mm) with sandblasting and heat treatment were used for the biaxial flexure test using a piston-on-three-ball biaxial fixture according to ISO 6872:1995[24]. Disk specimen was supported on three ball spheres (3.2 mm in diameter) equally spaced along a diameter of 10 mm and center-loaded by a steel piston (with a flat area of 1.1 mm in diameter ground along the contact surface) until fracture occurred at a crosshead speed of 0.5 mm/min. Failure stress was calculated using the equation listed in ISO 6872 with Poisson's ratio value of 0.25 for both materials:

$$S = \frac{-0.2387P(X-Y)}{d^2} \quad (5)$$

where S is the maximum center tensile stress in MPa and P the total load causing fracture in N;

$$X = (1+\nu)\ln(r_2/r_3)^2 + [(1-\nu)/2](r_2/r_3)^2 \quad (6)$$

$$Y = (1+\nu)[1+\ln(r_1/r_3)^2] + (1-\nu)(r_1/r_3{}^2) \quad (7)$$

where ν is Poisson's ratio, r_1 the radius of support circle, r_2 the radius of loaded area, r_3 the radius of specimen, and d the specimen thickness at fracture origin.

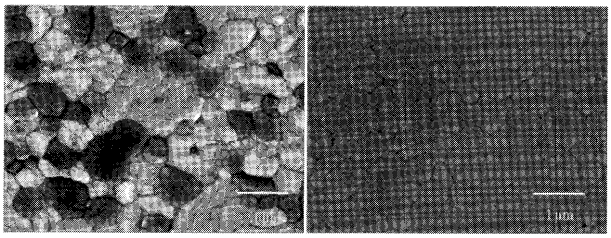

Fig. 1 SEM images of zirconia surfaces with thermal etching.

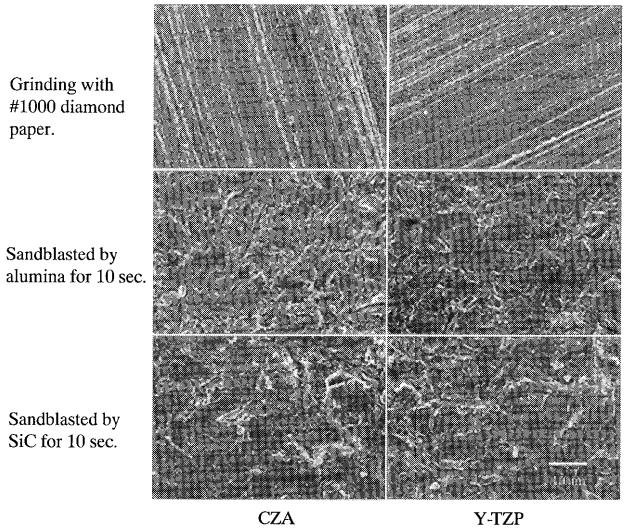

Fig. 2 SEM images of zirconia surfaces after grinding and sandblasting by alumina and SiC for 10 sec..

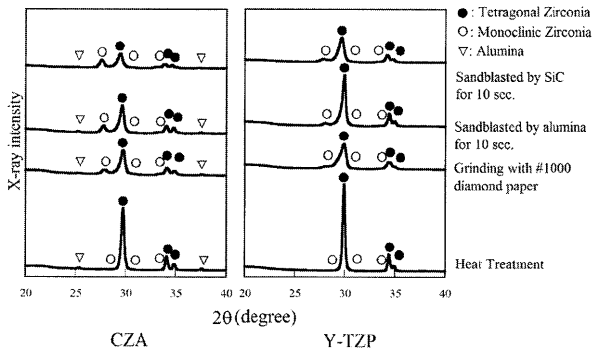

Fig. 3 XRD patterns of zirconia after grinding, sandblasting by alumina and SiC for 10 sec., and heat treatment.

RESULTS

Figure 1 shows the SEM images of CZA and Y-TZP surfaces. CZA was composed of 10 mol% CeO_2-stabilized TZP (white grains) as the matrix and 30 vol% of Al_2O_3 (black grains) as the second phase. Y-TZP consisted of homogeneous grains of an average

Table 2 Surface roughness values of zirconia after grinding and sandblasting by alumina and SiC for 10 and 90 seconds (mean±SD in μm)

Material	CZA		Y-TZP	
Parameter	Ra	Rz	Ra	Rz
grinding	0.33±0.12	1.90±0.89	0.30±0.04	1.62±0.41
alumina-sand-10 s	0.60±0.15	2.87±0.45	0.47±0.09	2.68±0.39
alumina-sand-90 s	0.56±0.06	4.31±0.63	0.68±0.08	4.61±0.78
SiC-sand-10 s	1.18±0.08	5.08±0.34	1.09±0.09	4.94±0.40
SiC-sand-90 s	0.96±0.11	6.12±0.53	0.84±0.06	5.40±0.40

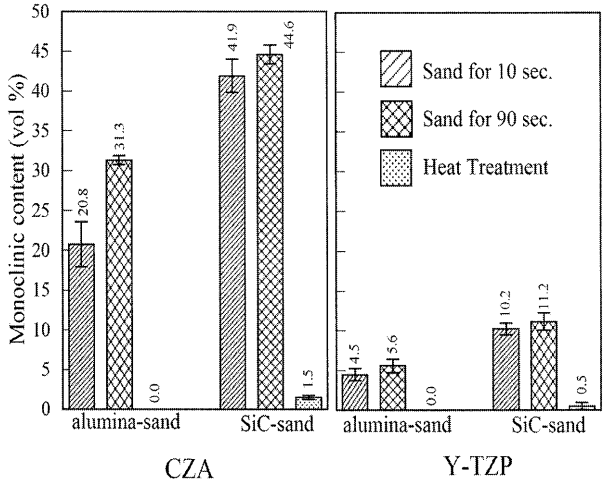

Fig. 4 Monoclinic ZrO_2 contents with sandblasting and heat treatment.

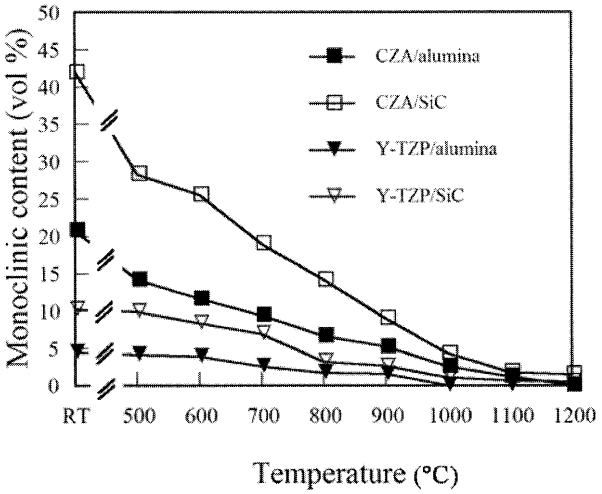

Fig. 5 Changes in monoclinic ZrO_2 contents with temperature of heat treatment.

size of 0.32 μm.

Figure 2 shows the SEM images of CZA and Y-TZP surfaces after grinding and sandblasting by alumina and SiC for 10 seconds. After grinding, many uniformly oriented scratches were observed on the surfaces of both zirconia types. With 70-μm alumina sandblasting, the surface altered to one covered with many grooves and voids, resulting in the disappearance of the scratches. With 125-μm SiC sandblasting, larger grooves and voids were observed on the surfaces of both zirconia types. Table 2 summarizes the surface roughness values of Ra and Rz for both zirconia types. It could be seen that for both zirconia types, sandblasting by SiC resulted in surface roughness values larger than those by alumina ($p<0.01$).

Figure 3 shows the XRD patterns of both zirconia types after grinding, sandblasting by alumina and SiC for 10 seconds, and heat treatment. In comparison to the XRD patterns after heat treatment, the diffraction peaks due to monoclinic ZrO_2 increased with grinding and both sandblasting methods. Conversely, the peaks for tetragonal ZrO_2 decreased and shifted to a lower degree.

Figure 4 shows the monoclinic ZrO_2 content derived from the XRD patterns using Eqs. (1) and (2). Between zirconia types, the monoclinic ZrO_2 content of CZA was larger than that of Y-TZP in each condition ($p<0.01$). Between sandblasting methods, the monoclinic ZrO_2 contents of both zirconia types after SiC sandblasting were larger than those with alumina sandblasting ($p<0.01$). Between sandblasting durations, the monoclinic ZrO_2 contents of both zirconia types were larger after being sandblasted for 90 seconds as compared to those of 10 seconds only ($p<0.05$). After heat treatment at 1200℃ for five minutes, the monoclinic ZrO_2 contents of both zirconia types decreased dramatically.

Figure 5 shows the changes in monoclinic ZrO_2 content of both zirconia types after being sandblasted by alumina and SiC for 10 seconds as a function of heat treatment temperature. Monoclinic ZrO_2 content decreased gradually with increase in temperature and dropped to approximately 1% after 1200℃.

Figure 6 shows the Raman spectrum of CZA. Figure 7 shows the monoclinic ZrO_2 contents and the equilibrium stress values derived from Raman spectrogram using Eqs. (3) and (4) as a function of

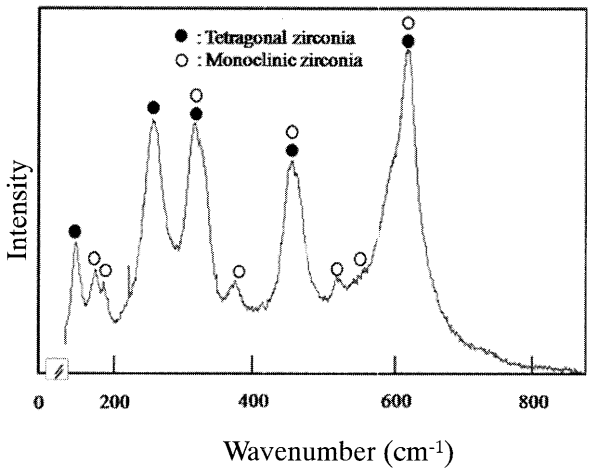

Fig. 6 Raman spectrum of CZA.

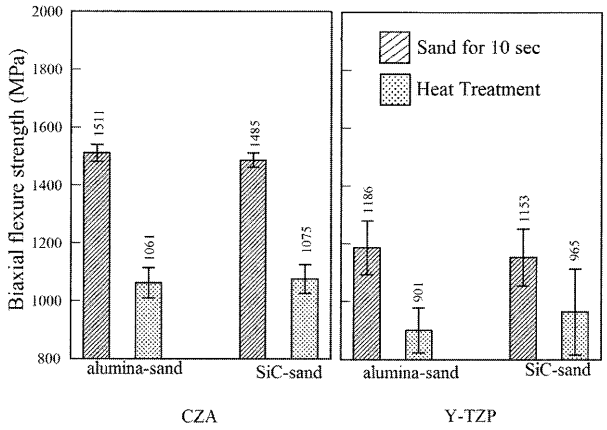

Fig. 8 Biaxial flexure strengths after sandblasting and heat treatment.

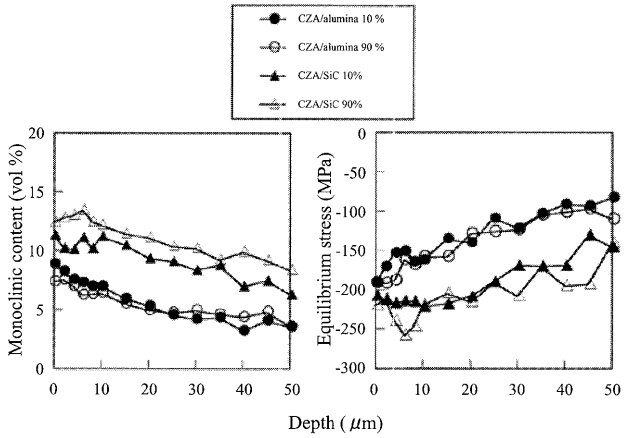

Fig. 7 Monoclinic ZrO_2 contents and equilibrium stress values derived from Raman spectroscopy analysis.

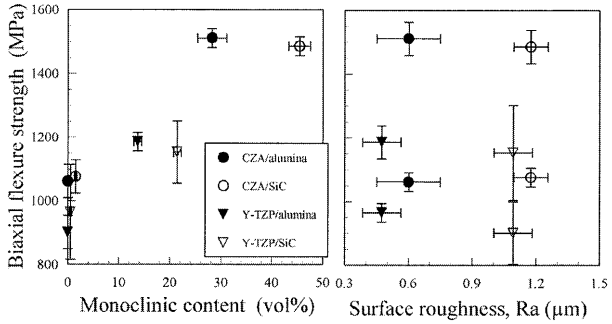

Fig. 9 Relationship between biaxial flexure strengths and monoclinic contents and surface roughness (Ra).

depth from the sandblasted surface. Monoclinic ZrO_2 contents and equilibrium stress values of both zirconia types sandblasted by SiC were larger than those by alumina ($p<0.01$). Both monoclinic ZrO_2 content and equilibrium stress gradually decreased from 10 μm with increase in depth. This seemed to be caused by the detection limitation of the decrease, although the laser beam focused on a specific depth. The differences in monoclinic ZrO_2 content between XRD analysis and Raman spectroscopy might be due to differences in wavelength and incidence angle.

Figure 8 shows the biaxial flexure strengths of both zirconia types after being sandblasted by alumina and SiC for 10 and 90 seconds and heat treatment. The biaxial flexure strength of CZA was higher than that of Y-TZP in each condition ($p<0.05$). Between sandblasting methods, the biaxial flexure strengths of both zirconia types sandblasted by SiC were slightly lower than those by alumina ($p>0.05$). After heat treatment, the biaxial flexure strengths of both zirconia types remarkably decreased.

Figure 9 shows the relation between biaxial flexure strength and monoclinic content and surface roughness (Ra). With increase in monoclinic ZrO_2 content, the biaxial flexure strength also increased. On the other hand, there was no clear relationship between biaxial flexure strength and surface roughness.

DISCUSSION

In light of the results obtained in this study, it could be concluded that the mechanical properties of zirconia were strongly influenced by the monoclinic ZrO_2 content. Similar results with Y-TZP have been previously reported by various researchers[12-16]. Swain *et al.*[25] suggested that volume expansion due to phase transformation from tetragonal to monoclinic ZrO_2 induced compressive stresses (σ_R) in the surface, and a hypothetical equation as follows was proposed:

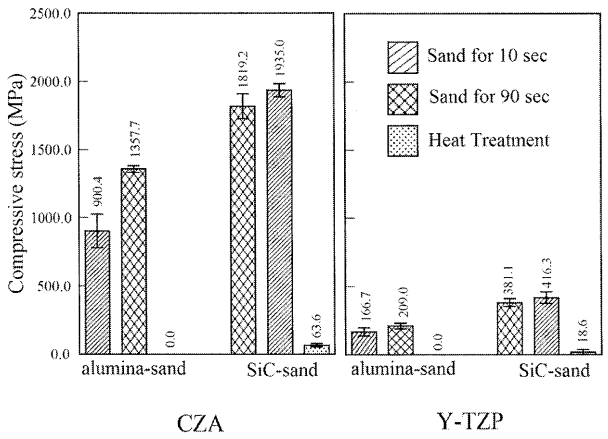

Fig. 10 Theoretical compressive stress values of zirconia calculated from the transformed monoclinic ZrO_2 contents in the surface.

$$\sigma_R = \frac{\Delta V \cdot V_m \cdot E}{3(1-\nu)} \quad (8)$$

where ΔV is volume expansion due to phase transformation at approximately 4%, V_m the monoclinic content, E the inherent elastic modulus of CZA or Y-TZP (240 and 210 GPa, respectively), and ν the Poisson's ratio (0.25 for both zirconia types).

Figure 10 shows the calculated results derived from the results of Fig. 4 using Eq. (8). This study revealed that, although the monoclinic ZrO_2 content after SiC sandblasting was larger than that after alumina sandblasting ($p<0.01$), the biaxial flexure strength after SiC sandblasting was lower than that after alumina sandblasting. Moreover, Raman analysis showed that the transformation zone depth[26] (TZD) in this study was determined to be approximately less than 10 μm. It could be assumed that excessive transformation from tetragonal to monoclinic ZrO_2 reduced the mechanical properties[27]. This effect might also influence the lifetime of zirconia[28,29]. To assess this hypothesis, further study is needed.

After sandblasting, CZA showed a higher content of transformed monoclinic ZrO_2 and higher biaxial flexure strength than Y-TZP. As shown in Fig. 1, CZA had an interpenetrated intragranular microstructure, where submicron-sized Al_2O_3 particle were dispersed among submicron-sized ZrO_2 grains. Several 10−100-nm Al_2O_3 particles were trapped within the ZrO_2 grains, and several 10-nm ZrO_2 particles were trapped within the Al_2O_3 grains. It was reported that the toughening and strengthening of ZrO_2-Al_2O_3 multiphase ceramics is mainly due to the dispersion of Al_2O_3[30]. Indeed, the strengthening mechanism of CZA could be ascribed to two factors. The first was related to decrease in flaw size due to reduced grain sizes for both ZrO_2 and Al_2O_3 grains, which is associated with interpenetrated intragranular nanodispersion. Consequently, several 10−100-nm sized inclusions were believed to have a role in dividing a grain size into finer sized particles by forming sub-grain boundaries[4]. The second was related to the stress-induced transformation underlying the strengthening mechanism of TZP ceramics. The retention of the tetragonal phase is critically governed by the grain size. In other words, reduced grain size is predicted to increase the critical stress that induces the tetragonal-monoclinic transformation. Taken together, these interactive contributions culminated in improved strength of CZA.

The biaxial flexure strengths of both zirconia types increased with increase in monoclinic ZrO_2 content (which was induced by sandblasting), but decreased with decrease in monoclinic ZrO_2 content (which was induced by heat treatment). This meant that the mechanical properties of zirconia were strongly affected by the stress-induced transformation. It is known that the stress-induced transformation of zirconia — *i.e.*, transformation from tetragonal to monoclinic phase — causes plastic deformation, thereby leading to high fracture toughness[31]. As shown in Fig. 7, the transformed zone was only 10 μm, although there was presence of the transformed monoclinic phase toward the interior in a decreasing trend. Thickness of the transformed layer mainly depends on the kind of sandblasting particles, but not on sandblasting time.

The fabrication of zirconia-based dental restorations entails a series of procedures including cutting, grinding, polishing, sandblasting, heat treatment after sandblasting, and firing for veneering porcelain[6-14]. Thus, it should be noted whether zirconia can maintain its mechanical properties even after these procedures. Against this background, restoratives made with zirconia should be designed based on the minimum strength, such as that yielded after heat treatment.

CONCLUSIONS

Investigation on surface and heat treatments in this study showed that CZA was more susceptible to stress-induced transformation than Y-TZP, and therefore showed higher biaxial flexure strength. This was probably due to their differences in microstructure. Monoclinic ZrO_2 content and biaxial flexure strength of CZA and Y-TZP increased with sandblasting, but decreased with heat treatment. Furthermore, the monoclinic ZrO_2 contents of both zirconia types after SiC sandblasting were larger than those after alumina sandblasting. Conversely, there were no significant differences in biaxial flexure

strength between SiC sandblasting and alumina sandblasting.

ACKNOWLEDGEMENTS

The present study was partially supported by a Grant-in-aid for General Scientific Research [(B) 18390521] from the Japan Society for the Promotion of Science and by a Research Grant for Young Scientist in Oral Biology from Kagoshima University Dental School. The authors also wish to express their appreciation to Matsushita Electric Works, Ltd. for their kind supply of zirconia specimens.

REFERENCES

1) Anusavice KJ. Philips' science of dental materials, 11th ed, Saunders-Elsevier Science, St Louis, 2003, pp.680-718.
2) Garvie RC, Hannink RH, Pascoe RT. Ceramic steel? Nature 1975; 258: 703-704
3) Piconi C, Maccauro G. Zirconia as a ceramic biomaterial. Biomaterials 1999; 20: 1-25.
4) Nawa M, Nakamoto S, Sekino T, Niihara K. Tough and strong Ce-TZP/alumina nanocomposites doped with titania. Ceramics International 1998; 24: 497-506.
5) Sato T, Shimada M. Transformation of ceria-doped tetragonal zirconia polycrystals by annealing in water. Am Ceram Soc Bull 1985; 64: 1382-1384.
6) Filser F, Kocher P, Weibel F, Lüthy H, Schärer P, Gauckler LJ. Reliability and strength of all-ceramic dental restorations fabricated by direct ceramic machining (DCM). Int J Compt Dent 2001; 4: 89-106.
7) Miyazaki T, Hotta Y, Kunii J, Fujiwara T. Current status and future prospects of a dental CAD/CAM system used in crown-bridge restorations. Dentistry in Japan 2007; 43: 189-194.
8) Reed JS, Lejus AM. Effect of grinding and polishing on near-surface phase transformations in zirconia. Mat Res Bull 1977; 12: 949-954.
9) Chevalier J. What future for zirconia as a biomaterial? Biomaterials 2006; 27: 535-543.
10) Deville S, Chevalier J, Gremillard L. Influence of surface finish and residual stresses on the ageing sensitivity of biomedical grade zirconia. Biomaterials 2006; 27: 2186-2192.
11) Denry IL, Holloway JA. Microstructural and crystallographic surface changes after grinding zirconia-based dental ceramics. J Biomed Mater Res Part B: Appl Biomater 2006; 76B: 440-448.
12) Luthardt RG, Holzhüter M, Sandkul O, Herold V, Schnapp JD, Kuhlisch E, Walter M. Reliability and properties of ground Y-TZP-zirconia ceramics. J Dent Res 2002; 81: 487-491.
13) Guazzato M, Quach L, Albakry M, Swain MV. Influence of surface and heat treatments on the flexural strength of Y-TZP dental ceramics. J Dent 2005; 33: 9-18.
14) Kosmač T, Oblak Č, Jevnikar P, Funduk N, Marion L. Strength and reliability of surface treated Y-TZP dental ceramics. J Biomed Mater Res: Appl Biomater 2000; 53: 304-313.
15) Kosmač T, Oblak Č, Jevnikar P, Funduk N, Marion L. The effect of surface grinding and sandblasting on flexural strength and reliability of Y-TZP zirconia ceramics. Dent Mater 1999; 15: 426-433.
16) Kosmač T. The effect of dental grinding and sandblasting on the biaxial flexural strength and Weibull modulus of tetragonal zirconia. Key Engin Mater 2004; 254-256: 683-686.
17) VITA VM9 working instructions. http://www.vita-zahnfabrik.com/resourcesvita/shop/en/en_3050430.pdf.
18) Garvie RC, Nicholson PS. Phase analysis in zirconia systems. J Am Ceram Soc 1972; 55: 303-305.
19) Toraya H, Yoshimura M, Sōmiya S. Calibration curve for quantitative analysis of the monoclinic-tetragonal ZrO_2 system by X-ray diffraction. J Am Ceram Soc 1984; 67: C119-C121.
20) Katagiri G, Ishida H, Ishitani A, Masaki T. Direct determination by a Raman microprobe of the transformation zone size in Y_2O_3 containing tetragonal ZrO_2 polycrystals. Advances in Ceramics 1988; 24: 537-544.
21) Yamada K, Nawa M, Pezzotti G. Confocal Raman spectroscopic analysis of phase transformation and residual stresses in Ce-TZP/Al_2O_3 nanocomposite for biomedical applications. Key Engin Mater 2007; 330-332: 373-376.
22) Pezzotti G. *In situ* study of fracture mechanisms in advanced ceramics using fluorescence and Raman microprobe spectroscopy. J Raman Spectrosc 1999; 30: 867-875.
23) Pezzotti G, Sakakura S. Study of the toughening mechanisms in bone and biomimetic hydroxyapatite materials using Raman microprobe spectroscopy. J Biomed Mater Res 2003; 65A: 229-236.
24) Ban S, Anusavice KJ. Influence of test method on failure stress of brittle dental materials. J Dent Res 1990; 69: 1791-1799.
25) Swain MV. Grinding-induced tempering of ceramics containing metastable tetragonal zirconia. J Mater Sci 1980; 15: 1577-1579.
26) Kosmač T, Wagner R, Claussen N. X-ray determination of transformation depths in ceramics containing tetragonal ZrO_2. J Am Ceram Soc 1981; 64: C72-73.
27) Ban S, Sato H, Suehiro Y, Nakanishi H, Nawa M. Effect of sandblasting and heat treatment on biaxial flexure strength of the zirconia/alumina nanocomposite. Key Engin Mater 2007; 330-332: 353-356.
28) Chevalier J, Olagnon C, Fantozzi G. Subcritical crack propagation in 3Y-TZP ceramics: static and cyclic fatigue. J Am Ceram Soc 1999; 82: 3129-3138.
29) Studart AR, Filser F, Kocher P, Gauckler LJ. *In vitro* lifetime of dental ceramics under cyclic loading in water. Biomaterials 2007; 28: 2695-2705.
30) Yu MQ, Fan SG, Shen Q, Zhang LM. Toughening and strengthening mechanism of zirconia-alumina multiphase ceramics. Key Engin Mater 2003; 249: 167-170.
31) Hasegawa H, Ozawa M. Strengthening mechanism of ceria-doped tetragonal zirconia polycrystals by heat treatment in reducing atmosphere. J Ceram Soc Jpn 2003; 111: 252-256.